PROF. D. O. SHAH

PROCEEDINGS

OF THE JOINT NSF-NIST

CONFERENCE ON NANOPARTICLES: SYNTHESIS, PROCESSING INTO FUNCTIONAL NANOSTRUCTURES, AND CHARACTERIZATION

12-13 MAY 1997

NATIONAL SCIENCE FOUNDATION
ARLINGTON, VIRGINIA

PREPARATION OF NANOPARTICLES OF SUPERCONDUCTING MATERIALS, MAGNETIC MATERIALS, AND SILVER HALIDES USING MICROEMULSIONS AS NANOREACTORS

B.J. Palla and D.O. Shah
NSF Engineering Research Center for Particle Science and Technology
Center for Surface Science and Engineering, Departments of Chemical Engineering and Anesthesiology, University of Florida, Gainesville, FL 32611, USA

ABSTRACT

Microemulsions are thermodynamically stable oil-water dispersions consisting of domains of oil and/or water stabilized by a film of surfactant molecules. The water-in-oil microemulsions were used as nanoreactors to induce the precipitation of cations. Using this approach, one can obtain particles in the range of 40 to 100 Angstrom in diameter. The interfacial rigidity appears to control the reaction rate in microemulsions. We have shown that the reaction rate is the slowest when the chain length of surfactant is equal to that of the oil plus co-surfactant alcohol molecules. The superconductors prepared from the nanopowders exhibit very large grain size, low porosity or high density, as well as better Meissner effect compared to the samples prepared from the conventional powders. The implications of preparing advanced materials from the nanopowders have been discussed.

INTRODUCTION

Current trends in many industries demand the production of ultrafine particles of decreasing size and increasing homogeneity. These potential technological applications have led to the development of several new techniques for the synthesis of nanoparticles in recent years. Liquid-phase techniques include bulk precipitation, sol-gel processing, spray-drying, and freeze-drying[1-5]; gas-phase techniques include gas evaporation-condensation, laser vaporization, and laser pyrolysis[6-10]; and vacuum synthesis techniques like sputtering, laser ablation, and ionized beam deposition.[11-14] These techniques often produce nanoparticles that have a wide particle size distribution, which is often not favorable for optimizing material characteristics.

The use of microemulsions as a media for the precipitation of ultrafine and monodisperse particles is based on the nature of the dispersed phase in the microemulsion. A microemulsion can be defined as a thermodynamically stable dispersion of two immiscible liquids consisting of microdomains of one or both liquids, stabilized by a monolayer of a surfactant system. The surfactant system serves to lower the interfacial tension between the dispersed and continuous phases to a low enough value ($<10^{-3}$ dynes/cm^2) to favor very small droplet formation, usually in

the 10-25 nm range. The surfactant system also serves to lower the interfacial viscosity of the droplets to a low enough value that collisions between droplets become inelastic, or sticky, in nature. The droplets of the dispersed phase in a microemulsion have been shown to possess a dynamic equilibrium, wherein droplets are constantly colliding, coalescing, and breaking apart. It is this dynamic nature of the droplets that facilitates exchange of material and hence chemical reaction within the dispersed phase.[15-16]

The first step in the process of developing a precipitation reaction in a microemulsion is the selection of a chemical reaction system that results in the precipitation of the desired product. The reactants selected must be soluble in the dispersed phase of the selected microemulsion system, and the reactants must be inert in this environment. The microemulsion system selected for the reaction must also be selected to achieve the most desirable properties of the product. The next step is to dissolve the reactants in the dispersed phase and produce two almost identical microemulsions, A and B, with the only difference between the microemulsions being the nature of the material dissolved in the dispersed phase. The microemulsions are then mixed, resulting in the desired precipitate, AB, being formed and limited in size by the microdomains of the dispersed phase. This process is illustrated in Figure 1. Reactions can also be carried out by adding a reducing agent or other reactive agent to the continuous phase of a single microemulsion with a second reactant dissolved in the dispersed phase.

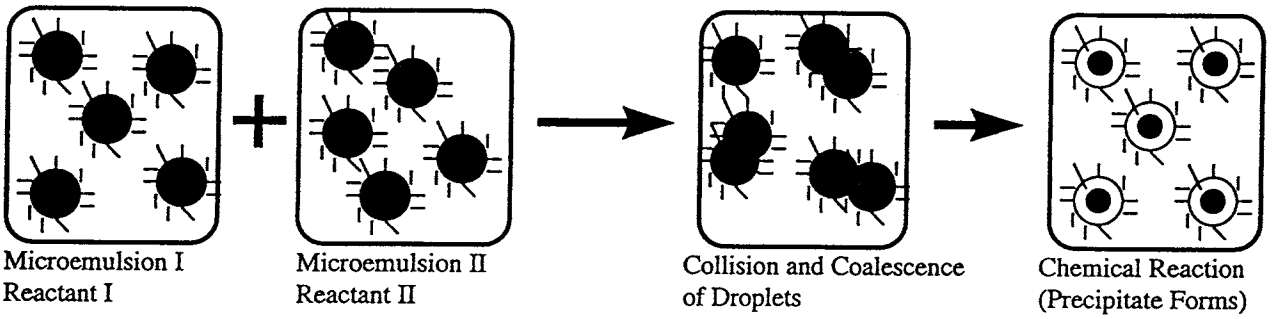

Figure 1. Schematic diagram showing the preparation of nanoparticles in microemulsions

The nature of reactions carried out using the microemulsion technique has been characterized extensively for many systems. The rate of reaction in the microemulsion depends on the microemulsion composition, structure of the various components of the microemulsion, and the hydrophobicity of the reactants.[17] For this reason, a particular microemulsion system should be thoroughly characterized with respect to dispersion droplet size and stability if an accurate prediction of the reaction product is to be made. Experimental results on reaction rates in microemulsions agree with current microemulsion stability theories when a component of the system is varied while keeping other parameters constant. Single parameter studies conclude that the reaction rate increases with increasing temperature and oil chain length, but decreases with increasing droplet size and water content, with no dependence on surfactant concentration.[15,18-19] Also, chain length compatibility among the co-surfactant, oil, and surfactant plays a significant role in determining the interfacial viscosity in the microemulsion system. When the carbon number of the surfactant is equal to the sum of the carbon numbers of the oil and the co-surfactant alcohol, the interfacial viscosity is increased significantly, and the reaction rate is

therefore reduced.[20-21] All of these parameters should be considered when selecting a microemulsion system for a reaction.

Due to the potential benefits of ultrafine, homogenous particles in numerous industries, research interest focusing on the use of the microemulsion reaction technique to produce nanoparticles has been steadily increasing. The use of microemulsions as a medium for the precipitation of ultrafine, monodisperse particles was first applied to the precipitation of the rare metals platinum, palladium, iridium, and rhodium. The metals were precipitated by reducing the corresponding salts dissolved in the aqueous phase of water-in-oil microemulsions by adding bulk hydrazine or hydrogen gas.[22] Laser and pulse radiolytic reduction was later used to produce colloidal gold in water-in-oil microemulsions. These particles have potential applications as condensers for electron storage in artificial photosynthesis.[23] Colloidal semiconductor particles are of great interest due to their unique photochemical and photophysical properties, and these properties are very much size dependent. Microemulsions have been used to produce monodisperse cadmium sulfide[24], lead sulfide[25], cadmium selenide[26], and silica-cadmium sulfide[27] semiconductor particles. Calcium carbonate, an important additive for lubricant oils, was produced by carbonation of its salt in the aqueous core of water-in-oil microemulsions.[28-30]

This paper will focus on the studies carried out in our laboratories on the production of nanoparticles of silver halides, superconductors, and magnetic materials using the microemulsion technology just described. Significant property improvements have been made to each of these particle systems by carrying out the reaction within the dispersed phase of a microemulsion.

PREPARATION OF NANOPARTICLES OF SUPERCONDUCTING MATERIALS

Nanoparticles of two different superconducting materials have been successfully produced by reaction in the cores of water-in-oil microemulsions. The materials produced by this technique have been shown to have exceptional properties when compared to materials produced by conventional techniques. By limiting the nucleation process during the chemical precipitation in a microemulsion, the particle size of the precipitated product is limited to the diameter of the dispersed phase droplet. Since there is only one thermodynamically favorable droplet size for any given microemulsion system, the particles will be monodisperse when precipitated. The decreased particle size and increased homogeneity of the nanoparticles produced by this technique result in a higher quality microstructure in the final sintered material, which leads to superior overall properties when compared to particles produced by the wet chemical methods.

Synthesis of Y-Ba-Cu-O (123) Superconductor

The Y-Ba-Cu-O (123) superconducting material was discovered after extensive efforts were made to improve the T_c of the first perovskite-like oxide superconductor, La-Ba-Cu-O.[31-33] The $YBa_2Cu_3O_{7-x}$ superconductor precursor powders have now been successfully prepared by reaction in the aqueous cores of water-in-oil microemulsions.[34-36] The microemulsion system selected for this reaction used octane as the hydrocarbon phase, water with dissolved salts as the aqueous phase, cetyl trimethyl ammonium bromide (CTAB) as the surfactant, and 1-butanol as

the co-surfactant. This system was selected because it has been shown that this microemulsion dissolves relatively large proportions of metal salt solutions such as $Y(NO_3)_3$ and $Cu(NO_3)_2$.[37] Initially, the yttrium, barium, and copper nitrates to be reacted had to be dissolved in the appropriate molar ratio (1:2:3) in the aqueous phase. However, to avoid errors due to an uncertainty in the water of crystallization associated with $Y(NO_3)_3$ and $Cu(NO_3)_2$, the starting solution was produced by dissolving Y_2O_3 and CuO in hot concentrated nitric acid (HNO_3) and later adding $Ba(NO_3)_2$. Ammonium oxalate, in 10% stoichiometric excess, was dissolved in water to form the other reactant phase. An initial reaction pH anywhere between 3.5 and 4.0 was found to yield monophasic YBCO on calcination, which is much less pH sensitive than the conventional coprecipitation method. This pH is achieved by using the concentrated nitric acid to dissolve the salts initially. The microemulsions were formulated as listed in Table 1.

Table 1: Composition of the microemulsions used for the Y-Ba-Cu-O precursor reaction

	Surfactant Phase	Hydrocarbon Phase	Aqueous Phase
Microemulsion I	CTAB + 1-butanol	n-octane	(Y,Ba,Cu) nitrate solution, Total metal conc.=0.3 N
Microemulsion II	CTAB + 1-butanol	n-octane	Ammonium oxalate solution, 0.45 N
Weight Fraction (for both I and II)	29.25%	59.42%	11.33%

The (Y,Ba,Cu) oxalate precipitate was separated from the oil and surfactant by centrifuging and washing with a 1:1 mixture of ethanol and chloroform, followed by pure ethanol. Once the surfactant was washed off, interparticle coagulation occurred to some extent. However, the precipitated oxalate particles produced by this method were still substantially smaller than those produced by conventional bulk methods. The particles were extensively characterized and compared to those produced by the conventional coprecipitation reaction. The results of this characterization are shown in Table 2.

Table 2: Comparison of physical properties of YBCO superconductor prepared by conventional aqueous phase precipitation vs. preparation by microemulsion reaction

Physical Property	Microemulsion Reaction	Conventional Reaction
ESD of (Y,Ba,Cu) oxalate precipitate	47.4 nm	380.6 nm
ESD of YBCO Powder Calcined at:	274.8 nm 820°C, 2 h	626.6 nm 860°C, 6 h
Grain size of YBCO pellet (from SEM): Sintered at:	15-50 μm 925°C, 12 h	0.5-2.0 μm 925°C, 12 h
Density of sintered pellet (fraction of single crystal density)	98 (±3)%	90 (±2)%
Magnetic susceptibility of Field-cooled sintered pellet (demagnetization corrected)	-10.95×10^{-3} (emu cm^{-3})	-3.06×10^{-3} (emu cm^{-3})
Magnetic susceptibility of Zero-Field-cooled sintered pellet (demagnetization corrected)	-72.05×10^{-3} (emu cm^{-3})	-11.43×10^{-3} (emu cm^{-3})
Fraction of ideal Meissner signal ($-1/4\pi$)	90.5%	14.4%
Superconducting T_c	93 K	91 K

Overall, the superconducting pellets produced by the microemulsion reaction were superior to those produced by the conventional reaction. Table 2 shows that the equivalent spherical diameter (ESD) of the particles of the both the dried oxalate precursor and the calcined oxide were significantly smaller for the microemulsion method. Also, the calcining temperature and time necessary for complete conversion of the oxalate to the oxide is lower for the microemulsion method. However, the calcined microemulsion product does not exhibit Meissner effect, and hence superconductivity, down to 4 K, while the calcined conventional product does display a weak Meissner effect. The true advantage of the microemulsion product only becomes evident after sintering as pellets (3 mm diameter, 1 mm thick, applied uniaxial pressure = 1.2 Gpa). Table 2 shows that the grain size of the sintered microemulsion product was 30-100 times larger than that of the sintered conventional product, as viewed by SEM. This results in a much higher theoretical density for the microemulsion product. Since grain boundaries are viewed as flaws from a standpoint of superconducting properties, the microemulsion product is far superior, because of less total grain boundary area. This is evident from the magnetic susceptibility measurements. The temperature dependence of the DC susceptibility was measured down to 4.2 K under a field of 23 G. The microemulsion-derived material exhibited substantially larger zero-field-cooled and field-cooled signals. The fraction of the ideal Meissner signal is therefore much larger for the samples prepared by the microemulsion method.

Synthesis of Bi-Pb-Sr-Ca-Cu-O Superconductor

As compared to the YBCO superconductor, even larger T_c values have been obtained in the 5-component systems Bi-Sr-Ca-Cu-O[38] and Ti-Ba-Ca-Cu-O[39] systems. This led to an investigation into making similar superconductors by microemulsion precipitation, which resulted in the successful production of Pb-doped Bi-Sr-Ca-Cu-O (2223) superconductor.[40] The Pb-doping is used to promote the formation of the high T_c phase, the formation of which is still not well understood.[41-45] After carrying out the appropriate reaction in the dispersed phase of a microemulsion, the final superconducting product exhibited superior properties to the conventional product. It should be emphasized that the precipitation of 5 cations in the desired ratios in bulk aqueous solution is very difficult due to the different solubilities in water.

The microemulsion system selected for this reaction consisted of cyclohexane as the hydrocarbon phase, water with dissolved salts as the aqueous phase, and Igepal CO-430 (nonylphenoxypoly (ethyleneoxy) ethanol) as the surfactant (no co-surfactant needed). Bismuth oxide, lead acetate, strontium carbonate, calcium carbonate, and copper acetate were dissolved in the molar cation ratio of 1.84:0.34:1.91:2.03:3.06 in a 25:75 (v/v) acetic acid/water mixture, then dried and dissolved again in a 50:50 (v/v) acetic acid/water mixture. Oxalic acid in 10% stoichiometric excess was dissolved in 50:50 (v/v) acetic acid/water mixture. These two aqueous phases were used in the microemulsion formulation shown in Table 3. The precursor oxalate particles were then separated in a superspeed centrifuge at 5000 rpm for 10 min and washed repeatedly with a 1:1 methanol:chloroform mixture to remove all surfactant. A JEOL-200 CX TEM picture of the dried powder revealed fairly monodisperse particles in the size range of 2-6 nm.

Table 3: Composition of the microemulsions used for the Bi-Pb-Sr-Ca-Cu-O precursor reaction

	Surfactant Phase	Hydrocarbon Phase	Aqueous Phase
Microemulsion I	Igepal CO-430	Cyclohexane	Solution of metal salts in acetic acid/water mixture
Microemulsion II	Igepal CO-430	Cyclohexane	Solution of oxalic acid in acetic acid/water mixture
Amount Used	15 g	50 mL	10 mL

The precursor powder was calcined at 800°C for 12 h, and energy dispersive x-ray analysis confirmed the presence of all the metal species in the original cationic ratio, and uniform mixing. The calcined powder was pressed into a pellet of 6 mm diameter under a static pressure of 120 Mpa and sintered at 850°C for 96 h. The DC magnetic susceptibility measurements revealed an abrupt change in the magnetization curve at 112 K, indicating the transition to superconducting state. The zero-field-cooled signal corresponds to 93% of the ideal Meissner shielding ($-1/4\pi$). X-ray powder diffraction spectra revealed almost phase pure 2223 oxide superconductor. Due to the ultrafine nature of the precursor powder, a larger grain growth and densification was observed. The density of the sintered sample, as determined by helium pycnometry, was 97% of the theoretical value.

In summary, both the YBCO and Bi-Pb-Sr-Ca-Cu-O superconductors obtained from microemulsion precipitation reaction were superior in nature to those obtained via conventional methods. The fraction of the ideal Meissner shielding, grain size, and fraction of theoretical density were all much larger for the microemulsion technique, due primarily to the ultrafine, homogeneous nature of the precursor powder precipitated in the constrained media. These results demonstrate the quality of material that can now be obtained in ultrafine, monodisperse form by precipitation in the aqueous cores of water-in-oil microemulsions.

PREPARATION OF NANOPARTICLES OF MAGNETIC MATERIALS

Nanoparticles of magnetic materials are the subject of intense research because of potential applications in the field of high-density magnetic recording and as constituents of magnetic fields.[46] There are certain magnetic oxides that are commonly used in modern processes for magnetic recording. These include γ-Fe_2O_3, Fe_3O_4, cobalt-modified Fe_2O_3, and CrO_2 for longitudinal recording and barium ferrite ($BaFe_{12}O_{19}$) and other hexagonal ferrites for high-density perpendicular recording. For these materials to function properly for recording purposes, the particles should be single domain, i.e. all the magnetic moments in the particle should be in one direction, and both the particle size and shape are crucially important.[47] For any magnetic material there exists a critical size, d_{SD}, below which it remains single domain. Also, there exists a characteristic size of the particle, d_{SP}, below which the material becomes superparamagnetic. Therefore, the size range over which the particle is useful in a storage medium is $d_{SP}<d<d_{SD}$. The same new techniques have been applied to producing nanoparticles of magnetic materials as listed in the introduction, but homogeneity of nanoparticles continues to be a problem with these methods. As a result, the microemulsion precipitation technique has been attempted as a means of producing uniform nanoparticles. Nanoparticles of magnetite[48-49] and maghemite[50] have been

previously prepared using this technique. This section of the paper focuses on the preparation of barium ferrite, γ-Fe_2O_3, and cobalt-modified Fe_2O_3 by the microemulsion technique.

Synthesis of Barium Ferrite ($BaFe_{12}O_{19}$)

Barium ferrite has traditionally been used in permanent magnets because of its high intrinsic coercivity and fairly large crystal anisotropy.[51] However, more recently, it has emerged as a leading material for use in high density perpendicular recording.[52] The classical ceramic method for the preparation of barium ferrite consists of firing mixtures of iron oxide and barium carbonate at temperatures near 1200°C, but these particles must then be ground below the critical size, d_{SD}, so that they are single domain. This grinding process results in an inhomogeneous final product with low coercivity.[53-56] More modern techniques of nanoparticulate production improve upon, but do not conquer, the problem of polydispersity in the final magnetic particles. The microemulsion precipitation technique has proven superior to the other methods in producing barium ferrite particles.[36,57-58]

The microemulsion system selected for the precipitation of barium ferrite used n-octane as the hydrocarbon phase (44% by wt.), cetyl trimethyl ammonium bromide (CTAB) as the surfactant (12% by wt.), n-butanol as the co-surfactant (10% by wt.), and a salt solution as the dispersed aqueous phase (34% by wt.). The aqueous solution in one microemulsion contained a mixture of barium nitrate and ferric nitrate as the dissolved salt, while the other microemulsion contained the precipitating agent, ammonium carbonate. Upon mixing the two microemulsions, barium-iron carbonate precipitated within the nano-size droplets of the microemulsion. The particles were separated in a centrifuge at 5000 rpm for 10 minutes, and washed in a 1:1 mixture of methanol and chloroform followed by pure methanol to remove any oil and surfactant from the particles. The precipitate was dried at 100°C and then calcined at 950°C for 12 hours to insure complete conversion of the carbonate precursor into barium ferrite ($BaFe_{12}O_{19}$).

The calcined particles were found by TEM to have a mean particle size in the range of 50-100 nm, while the precursor particles were in the range of 5-15 nm, indicating that growth took place during calcination. X-ray diffraction showed all characteristic peaks for barium ferrite. Room temperature magnetic property measurements were carried out on a vibrating sample magnetometer (VSM) using an unoriented, random assembly of particles. The intrinsic coercivity (H_c) of the particles was found to be 5397 Oe, indicating that the particles were essentially single domain. The critical domain size, d_{SD}, was reported to be in the range of 1 μm for room temperature barium ferrite, so the particle size of under 100 nm indeed was in the single domain regime.[59]

Synthesis of γ-Fe_2O_3

A magnetic oxide commonly used for information storage[60], color imaging[61], bioprocessing[62], ferrofluids[63], magnetic refrigeration[64], and magnetic resonance imaging[65] is γ-Fe_2O_3. A microemulsion system similar to the one used for the synthesis of barium ferrite was used for the precipitation of γ-Fe_2O_3.[36,66] One microemulsion contained a 0.15 M solution of

ferrous sulfate as the aqueous phase. To this microemulsion a 2.0 M solution of tetra ethyl amine (TEA) in octane was added to hydrolyze the Fe^{2+} ions in the aqueous phase. The second microemulsion for the reaction contained sodium nitrite as the aqueous phase. After mixing, the precipitated iron oxide particles were treated in a manner similar to the barium ferrite particles to remove surfactant impurities. TEM revealed monodisperse, spherical particles in the size range of 22-25 nm, and X-ray diffraction confirmed characteristic peaks corresponding to γ-Fe_2O_3, with no impurities of α-Fe_2O_3 or Fe_3O_4.

The room temperature magnetization curve for the dried powder, obtained on a VSM, showed zero coercivity, indicating that the iron oxide particles were superparamagnetic at room temperature. This means that the particles prepared were below the characteristic size, d_{SP}, at which the particles become superparamagnetic. If microemulsions are used for in situ synthesis of γ-Fe_2O_3, the particles can be isolated easily in powder form for use in magnetic imaging. The powders can also be dispersed in aqueous or non-aqueous media for other applications such as ferrofluids. As a result, these particles can be made useful despite their superparamagnetic properties.

Synthesis of Cobalt Ferrite Particles ($CoFe_2O_4$)

The γ-Fe_2O_3 particles discussed in the previous section are commonly used for magnetic recording applications that do not require high recording densities. However, these iron oxides have a low intrinsic coercivity, which causes a serious limitation for high-density recording applications. As a result, modification methods have been developed that raise the coercivity of iron oxide particles from their typical value of 300-400 Oe to well above 1000 Oe. One of these methods is cobalt modification. The enhancement in coercivity with this method occurs because the cobalt ions impart an increased magnetocrystalline anisotropy to the oxide structure due to the coupling of spins of the cobalt ions with the iron ions. Cobalt-modified oxide particles are the predominant magnetic material used in video tapes today, and they are becoming more common in high-density digital recording of tapes and disks.[67-68] These particles have recently been successfully produced by the microemulsion precipitation technique of nanoparticle production.[69]

The microemulsion system selected for this reaction was similar to that used for the preparation of both barium ferrite and γ-Fe_2O_3 particles, except that the aqueous phase was modified to fit the reaction needed. One microemulsion contained an aqueous phase of 0.01 M cobalt (II) nitrate and 0.02 M ferric nitrate to facilitate the 1:2 molar ratio of Co^{2+}:Fe^{3+} needed for the final product. The other microemulsion contained an aqueous phase of ammonium hydroxide in a 10% stoichiometric excess for the reaction. The cobalt-iron hydroxide particles that precipitated when the microemulsions were mixed were treated in a similar manner to the barium ferrite and γ-Fe_2O_3 particles. The precursor hydroxide particles were then calcined at 600°C for 5 hours for complete conversion into the magnetic ferrite ($CoFe_2O_4$).

A TEM analysis of the calcined particles revealed particles less than 50 nm in size, which is below the reported critical domain size for cobalt ferrite. The calcined particles were spherical

in nature, which is expected due to the precursor particles being spherical. The precursor particles were 5-20 nm in size, which indicates that the calcination time and temperature are both important variables in controlling the size and growth of particles synthesized using microemulsions. An X-ray diffractogram of the particles indicated characteristic peaks for $CoFe_2O_4$ only. Magnetization measurements were performed on the particles and revealed a high coercivity of 1440 Oe. This high coercivity value indicates that the particles formed are indeed single domain, and furthermore, are above the superparamagnetic characteristic size, d_{SP}, unlike the γ-Fe_2O_3 particles discussed in the previous section. These results verify that the microemulsion technique can be successfully employed to produce high coercivity, monodisperse nanoparticles of cobalt ferrite.

Since the same microemulsion system was used in producing barium ferrite ($BaFe_{12}O_{19}$), γ-Fe_2O_3, and cobalt ferrite ($CoFe_2O_4$) nanoparticles, these results illustrate the versatility of the microemulsion technique. The only difference in the microemulsions was the dissolved salts in the aqueous phase, which determine the nature of the precipitate formed.

PREPARATION OF NANOPARTICLES OF SILVER HALIDES

Ultrafine particles of silver halides have been pursued because of applications in photographic emulsions.[36,70-71] However, these particles are extremely difficult to obtain in monodisperse form, which is essential for the application. Silver halides have been successfully prepared in ultrafine, monodisperse form by reaction in the aqueous cores of water-in-oil microemulsions.[72-74] Particles of both AgCl and AgBr were produced, and parameters were varied to study the effects on various properties of the particles.

Synthesis of Silver Chloride (AgCl)

Silver chloride was precipitated in the aqueous cores of a water-in-oil microemulsion by reacting silver nitrate and sodium chloride. The microemulsion system selected for this reaction used sodium di-2-ethylhexyl sulfosuccinate (AOT) as the surfactant, which requires no co-surfactant alcohol in forming microemulsions because of its nearly balanced hydrophile-lipophile property.[75-77] Different hydrocarbon phases were investigated with this system, including n-hexane, n-heptane, n-octane, n-nonane, n-decane, and n-dodecane. The aqueous phase in the first microemulsion was silver nitrate ($AgNO_3$, 0.4 M), while the aqueous phase in the second microemulsion was sodium chloride (NaCl, 0.4 M). The microemulsions had identical compositions and each solubilized 8 moles of aqueous phase per mole of surfactant (AOT, 0.15 M in alkane). The microemulsions were mixed under constant stirring to form AgCl particles in suspension.

The particles were thoroughly characterized. First, the particles were viewed under transmission electron microscope (TEM) to study the morphology and aggregation state of the microcrystals prepared from each hydrocarbon phase. In each case, the amount of hydrocarbon phase was kept constant. For all hydrocarbons investigated, the particle size of the precipitated particles was in the 5-10 nm range, and the particles were spherical and relatively uniform in

size. For n-heptane, the TEM pictures of the particles showed no aggregation at all 1 day and 1 week after initially mixing the reactant microemulsions. For n-dodecane, aggregation was not evident 4 hours after mixing, but it was evident 5 days after mixing. However, sonification easily broke up the weak aggregates, and the sonicated particles were of the same size as the initial particles. This verifies the stability of the dispersions, even after one week, which has been explained on the basis of a low attractive interaction between the microemulsion droplets containing the AgCl nanoparticles.

The microemulsions were also characterized by Quasi-elastic light scattering (QELS) in order to monitor the variation of the hydrodynamic diameter of the dispersions after mixing the microemulsions. By monitoring the scattered light intensity after mixing, the growth of the AgCl particles could be inferred from the hydrodynamic diameter. Using n-heptane as the hydrocarbon phase, it was found that both the hydrodynamic diameter and polydispersity remained almost constant initially and started to increase after approximately 100 minutes. This implies that, within the first 100 minutes, only a single mode of translational diffusion was observed. After that, a more significant contribution of AgCl microcrystals was observed. This means that in the first 100 minutes, the microcrystals were very small and restricted within the microemulsion droplets. However, after this initial stage, the microcrystals were no longer limited entirely to the "cages" of microemulsion droplets and thus the hydrodynamic diameter increased. This was because of a depletion of surfactant due to the adsorption of surfactant onto the newly created AgCl particle surfaces. This depletion of surfactant resulted in an increase in the hydrodynamic diameter of the droplets. These results imply the formation of loose aggregates after the initial stage. However, the TEM study for the n-heptane system verifies that any aggregates are very loosely bound in this system. Even after 1 week, aggregation was not evident by TEM for the n-heptane system.

The rate of formation of AgCl was also studied with microemulsion composition variations. The transmittance of the microemulsion was monitored after the reactant microemulsions were mixed. A stopped-flow photometry apparatus was used to provide rapid and homogeneous mixing, along with transmittance measurements after an indicator (potassium chromate) was added to one of the microemulsions. The transmittance of the dispersion decreased as the reaction progressed. By studying the reaction rate inside the microemulsion, the stability of the colloid was explored. A more rigid interface will slow the reaction rate, since droplets will not coalesce and allow the components to mix. Therefore, this apparatus was used to determine the effects of microemulsion components on reaction kinetics. The reaction rate was found to increase as the alkane chain length increased, the short chain alcohol concentration increased, and the alcohol chain length decreased. Also, the addition of a nonionic surfactant, Arlacel-20, decreased the reaction rate significantly.

Synthesis of Silver Bromide (AgBr)

The same microemulsion was used to prepare silver bromide as with silver chloride, except that the second microemulsion contained sodium bromide (NaBr), in place of sodium chloride. The particles produced from these microemulsions were also spherical and uniform in size. As the chain length of alkane used was increased from n-hexane to n-octane, the size

distribution of the particles increased from 5 to 10 nm. The solubilization of the aqueous phase in the microemulsion was also studied in this system versus hydrocarbon chain length and salt concentration. It was found that the maximum water solubilization decreased substantially as the NaBr or $AgNO_3$ concentration increased. It was also found the maximum water solubilization had a maximum when plotted versus hydrocarbon chain length. The location of the maximum was observed for a hydrocarbon chain length of about 8 for a pure water system and a chain length of about 13 for a 0.4 M NaBr system. These results point out the importance of characterizing a microemulsion system before attempting its use in a reaction in order to optimize the product properties obtained.

From these results, it is evident that the preparation of silver halide nanoparticles by microemulsion reaction has been investigated extensively. The resulting particles are monodisperse in nature, which is an improvement over the nanoparticles produced by other techniques.

CONCLUSIONS

Nanoparticles of superconducting materials, magnetic materials, and silver halides have been successfully produced using the microemulsion precipitation technique. By using this technique instead of other nanoparticle production techniques, the particles are uniform in both size and shape. The superconducting nanoparticles are monodisperse in nature, and therefore their sintered pellets have a high fraction of ideal Meissner shielding and theoretical density. The magnetic nanoparticles are also monodisperse, with exceptionally high intrinsic coercivity for the cobalt-modified iron oxide particles. Also, the silver halides are of uniform size and shape, which is an improvement over particles previously produced. The microemulsion precipitation technique has extraordinary potential for producing high quality nanoparticles of a wide variety. The potential for this exciting field has just started to unravel.

ACKNOWLEDGEMENTS

The authors want to thank the Engineering Research Center for Particle Science and Technology at the University of Florida (ERC), the National Science Foundation (grants #EEC-94-02989, CBT 8807321, and CTS 8922574), and the ERC Industrial Partners for the financial support provided for these projects.

REFERENCES

1. Veale, Fine Powders: Preparation, Properties and Uses (Halsted Press/Wiley, New York, 1972), p.1.
2. Goldman and A.M. Lang, J. Phys. Colloq., 297 (1987).
3. Kagawa, M. Kikuchi, R. Ohno and T. Nagae, J. Am. Ceram. Soc., 64 , C 7 (1981).
4. Matijevic, Langmuir, 2, 12 (1986).
5. Sugimoto, Adv. Coll. Interface Sci., 28, 65 (1987).
6. Uyeda, J. Cryst. Growth, 24, 69 (1974).
7. Liu, Q-L. Zhang, F.K. Tittel, R.F. Curl and R.E. Smalley, J. Chem. Phys., 85, 7434 (1986).
8. Morse, Chem. Rev., 86, 1049 (1986).
9. K LaiHing, R.G. Wheeler, W.L. Wilson and M.A. Duncan, J. Chem. Phys., 87, 3401 (1987).

10. Cannon, S.C. Danforth, J.H. Flint, J.S. Haggerty and R.A. Marra, J. Am. Ceram. Soc., 65, 324 (1982).
11. Fayet and L. Woste, Z. Phys. D, 3, 177 (1986).
12. Wright, J.K. Bates, and D.M. Gruen, Inorg. Chem., 17, 2275 (1978).
13. L. Mandich, V.E. Bondybey and W.D. Reents, J. Chem Phys., 80, 4245 (1987).
14. Takagi, Z. Phys. D, 3, 272 (1986).
15. Fletcher, A.M. Howe and B.H. Robinson. J. Chem. Soc. Faraday Trans. I, 83, 985 (1987).
16. Eicke, J.C.W. Shepherd and A. Steinemann. J. Colloid Interface Sci., 56, 168 (1976).
17. Minero, E. Pramauro and E. Pelizzetti, Colloids and Surfaces, 35, 237 (1989).
18. Moya, C. Izquierdo and J. Casado, J. Phys. Chem., 95, 6001 (1991).
19. Lang, N. Lalem and R. Zana, Colloids and Surfaces, 68, 199 (1992).
20. Chattopadhyay, D.O. Shah and L. Ghaicha, Langmuir, 8, 27 (1992).
21. Pillai and D.O. Shah, Dynamic Properties of Interfaces and Association Structure, (1996) p. 156.
22. Boutonnet, J. Kizling, P. Stenius and G. Maire, Colloids and Surfaces, 5, 209 (1982).
23. Kurihara, J. Kizling, P. Stenius and J.H. Fender, J. Am. Chem. Soc., 105, 2574 (1983).
24. Lianos and J.K. Thomas, Chem. Phys. Lett., 125, 299 (1986).
25. Eastoe and A.R. Cox, Colloids and Surfaces, 101, 63 (1995).
26. Steigerwald, J.M. Gibson, T.D. Harris, R. Kortan, A.J. Muller, A.M. Thayer, T.M. Duncan, D.C. Douglass and L.E. Brus, J. Am. Chem. Soc., 110, 3046 (1988).
27. Chang, L. Liu and S.A. Asher, J. Am. Chem. Soc., 116, 6739 (1994).
28. Kandori, K. Kon-no and A. Kitahara, J. Colloid Interface Sci., 122, 78 (1988).
29. Kandori, N. Shizuka, K. Kon-no and A. Kitahara, J. Disp. Sci. Tech. (1988).
30. Roman, P. Hoornaert, D. Faure, C. Biver, F. Jacquet and J.M. Martin, J. Colloid Interface Sci., 144, 324 (1991)
31. Bednorz and A. Muller, Z. Phys., B64, 189 (1986).
32. Wu, J.R. Ashburn, C.J. Torng, P.H. Hor, R.L. Meng, L. Gao, Z.J. Huang, Y.Q. Wang and C.W. Chu, Phys. Rev. Lett., 58, 908 (1987).
33. Tabagi, S. Uchida, K. Kishio, K. Kitazawa, K. Fueki, and S. Tanaka, Jpn. J. Appl. Phys., 26, L239 (1987).
34. Ayyub, A.N. Maitra and D.O. Shah, Physica C, 168, 571 (1990).
35. Kumar, V. Pillai, S.R. Bates and D.O. Shah, Mat. Lett., 16, 68 (1993).
36. Pillai, P. Kumar, M.J. Hou, P. Ayyub and D.O. Shah, Adv. Coll. Inter. Sci., 55, 241 (1995).
37. Ayyub, A.N. Maitra and D.O. Shah, J. Chem. Soc. Faraday Trans., 89, 3585 (1993).
38. Maeda, Y. Tanaka, M. Fukotonei and T. Asano, Jpn. J. Appl. Phys., 27, L209 (1988).
39. Sheng and A.M. Hermann, Nature, 332, 138 (1988).
40. Kumar, V. Pillai and D.O. Shah, Appl. Phys. Lett., 62, 765 (1993).
41. Sunshine, Phys. rev. B, 38, 893 (1988).
42. Yamada and S. Murase, Jpn. J. Appl. Phys., 27, L996 (1988).
43. Takano, J. Takada, K. Oda, H. Kitaguchi, Y. Miura, Y. Ikeda, Y. Tomic and H. Mazaki, Jpn. J. Appl. Phys., 27, L1041 (1988).
44. Mizuno, H. Endo, J. Tsuchiya, N. Kijima, A. Sumiyama and Y. Oguri, Jpn. J. Appl. Phys., 27, L1225 (1988).
45. Green, C. Jiang, Y. Mei, H.L. Luo and C. Politis, Phys. Rev. B, 38, 596 (1988).
46. Ozaki, MRS Bull., 12, 35 (1989).
47. Craik, Magnetic Oxides, Parts 1&2, (Wiley Interscience, New York, 1975), p.1.
48. Bandow, K. Kimura, K. Konno and A. Kitahara, Jpn. J. Appl. Phys., 26, 713 (1987).
49. Lee, C.M. Sorensen, K.J. Klabunde and G.C. Hadjipanayis, IEEE Trans. Magn., 28, 3180 (1992).
50. Ayyub, M.S. Multani, M. Barma, V.R. Palkar and R. Vijayaraghan, J. Phys. C: Solid State Phys., 21, 2229 (1988).
51. Cullity, Introduction to Magnetic Materials (Addison-Wesley Publishing Co., Massachusetts, 1972), p. 575.
52. Kubo, T. Ido, and H. Yokoyama, IEEE Trans. Magn., 18, 1122 (1982).
53. Kojima, in E.P. Wohlfarth (Ed.), Ferromagnetic Materials, Vol. 3 (North-Holland, Amsterdam, 1982), p. 305.
54. Bye and C.R. Howard, J. Appl. Chem. Biotechnol., 21, 319 (1971).
55. Haneda and H. Kojima, J. Am. Ceram. Soc., 57, 68 (1974).
56. Paulus, Preparative Methods in Solid State Chemistry (Academic Press, New York, 1972), p. 488.
57. Pillai, P. Kumar and D.O. Shah, J. Magn. Mag. Mater., 116, L299 (1992).
58. Pillai, P. Kumar, M.S. Multani and D.O. Shah, Colloids Surfaces A: Physicochem. Eng. Aspects, 80, 69 (1993).
59. Goto, M. Ito and T. Sakurai, Jpn. J. Appl. Phys., 19, 541 (1980).

60. Gunther, Phys. World, 3, 28 (1990).
61. Ziolo, U.S. Patent 4474866 (1984).
62. Nixon, C.A. Koval, R.D. Noble and G.S. Slaff, Chem. Mater., 4, 177 (1992).
63. Enton, I. de Sabata and L. Vekas, J. Magn. Mag. Mater., 85, 219 (1990).
64. McMichael, R.D. Shull, L.J. Swartzendruber, L.H. Bennet and R.E. Watson, J.Magn. Mag. Mater., 111, 29 (1992).
65. Fank and P.C. Lanterbur, Nature, 363, 334 (1993).
66. Chhabra, M Lal, A.N. Maitra, and P. Ayyub, Colloid & Polymer Science, 273, 939 (1995).
67. Bate, in: D.J. Craik (Ed.), Magnetic Oxides, Part 2, (Wiley Interscience, New York, 1975), p. 703.
68. Sharrock, IEEE Trans. Magn., 25, 4374 (1989).
69. Pillai and D.O. Shah, J. Magn. Mag. Mater., 163, 243 (1996).
70. Carroll, G.C. Higgins and T.H. James, Introduction to Photographic Theory: The Silver Halide Process (John Wiley and Sons, New York, 1980), p.1.
71. Locker, in R.E. Kirk, D.F. Othmer, M. Grayson and D. Eckroth (Eds.), Encyclopedia of Chemical Technology, 17 (John Wiley and Sons, New York, 1982), p. 611.
72. Chew, L.M. Gan and D.O. Shah, J. Disp. Sci. Tech., 11, 593 (1990).
73. Hou and D.O. Shah, in Y.A. Attia, B.M. Moudgil and S. Chander (Eds.), Interfacial Phenomena in Biotechnology and Materials Processing (Elsevier, Amsterdam, 1988), p. 443.
74. Dvolaitzky, R. Ober, C. Taupin, R. Anthore, X. Auvray, C. Petipas, and C. Williams, J. Disp. Sci., 4, 29 (1983).
75. Frank and G. Zografi, J. Coll. Interface Sci., 29, 27 (1969).
76. Kunieda and K. Shinoda, J. Coll. Interface Sci., 75, 601 (1980).
77. Shinoda and H. Kunieda, J. Coll. Interface Sci., 118, 586 (1987).